BULLETIN OF THE EARTHQUAKE
RESEARCH INSTITUTE
Vol. 45 (1967), pp. 299-312

16. *Attenuation of P Waves in the Upper and Lower Mantle.**

By Hiroo KANAMORI,

Earthquake Research Institute.

(Read Jan. 24, 1967.—Received March 31, 1967.)

Abstract

Difference of Q, specific quality factor, for P waves in the upper and the lower mantle is determined around the period of 1 sec by the spectral analysis of P, PcP, pP and $pPcP$ phases from nine aftershocks of the Alaska earthquake of March 28, 1964. The effects of crustal layerings are removed by Haskell's method. From relative spectral ratios P/PcP and $pP/pPcP$, the maximum of the average Q for P waves, $\bar{Q}_\alpha$, is estimated as 800. The ratio of the average Q for the upper 870 km of the mantle, $\bar{Q}'_\alpha$, to that for the rest of the mantle, $\bar{Q}''_\alpha$, cannot be larger than 0.3. The probable range of $\bar{Q}_\alpha$, $\bar{Q}'_\alpha$, $\bar{Q}''_\alpha$ and $\bar{Q}'_\alpha/\bar{Q}''_\alpha$ can be determined as $410<\bar{Q}_\alpha<630$, $180<\bar{Q}'_\alpha<240$, $1600<\bar{Q}''_\alpha<6000$, and $0.04<\bar{Q}'_\alpha/\bar{Q}''_\alpha<0.12$ respectively, when the previously determined relation between $\bar{Q}_\alpha$ and $\bar{Q}_\alpha/\bar{Q}_\beta$ ($\bar{Q}_\beta$; average Q for shear), and the range of the ratio $1.8\leqq\bar{Q}_\alpha/\bar{Q}_\beta\leqq2.5$ suggested by surface wave studies are used.

Introduction

The attenuation of seismic waves which is a manifestation of the earth's anelasticity has an important bearing on the state and the temperature of the deep interior. A variety of techniques have been applied in order to determine Q, the specific quality factor, of the earth. The quality and the significance of the individual result differ widely. Some of the results depend greatly on various assumptions which do not at first seem reasonable. In some other cases, although the involved assumptions are reasonable, the quality of the data is not good enough to permit an accurate determination of Q.

Our present knowledge of seismic wave attenuation in the earth's

* This work was done in part at the Seismological Laboratory, California Institute of Technology, Pasadena. (Contribution No. 1448, Division of Geological Sciences, California Institute of Technology.)

interior is not sufficient to establish the frequency dependence and the distribution with depth of Q, which are most pertinent to many geophysical problems.

The purpose of the present work is to determine the difference of Q for P waves in the upper and the lower mantle at periods around 1 sec. Although short-period waves are suited to the study of the earth's attenuative property, they are easily affected by various source effects, irregularities in the structure and noise. Therefore I attempted here to minimize these effects statistically by using a number of earthquakes from almost the same locality. Nine aftershocks of the Alaska earthquake of March 28, 1964 are used to determine the spectral difference between P and PcP phases and then to estimate the difference of Q_α in the upper and the lower mantle.

Data

Nine aftershocks of the Alaska earthquake of March 28, 1964 recorded at Tonto Forest Seismological Observatory, Arizona ($\Delta \doteqdot 35°$) by the short-period Johnson-Matheson seismograph are used. The instrument constants are; $Ts=1.25$ sec, $\lambda s=0.54$, $Tg=0.33$ sec, $\lambda g=0.61$, and $\sigma^2=0.09$.

Table 1 lists all the earthquakes used for the present analysis. The identification of the phases is based on the travel times. Fig. 1 shows all the pairs of P–PcP and pP–$pPcP$ reproduced from the seismograms.

Table 1. List of earthquakes

No.	Date	Origin Time G.C.T.	Lat.	Long.	Focal Depth	Mag. (C.G.S.)	Δ to TFO	P Arrival Time	$PcP-P$	$pPcP-pP$
		h m s						h m s	m s	m s
1	28 Mar. '64	06 08 44.2	60.1N	148.6W	20 km	5.6	35.4°	06 15 41.6	2 27.9	2 28.4
2	2 Apr. '64	11 41 10.7	58.8N	149.6W	20	5.4	35.2	11 48 06.2	2 29.4	2 29.7
3	5 Apr. '64	19 28 18.1	60.2N	146.7W	15	5.8	34.6	19 35 10.4	2 32.2	2 32.3
4	10 Apr. '64	01 08 00.2	58.4N	150.6W	15	5.5	35.5	01 14 58.9	2 27.6	2 28.4
5	17 Apr. '64	09 09 07.8	57.7N	151.4W	20	5.4	35.8	09 16 06.9	2 26.9	
6	16 May '64	14 44 54.0	57.6N	151.0W	33	5.4	35.4	14 51 49.6	2 28.0	
7	30 May '64	03 18 08.3	59.5N	148.5W	15	5.5	35.1	03 25 04.2	2 29.4	
8	11 July '64	20 25 40.3	59.7N	146.2W	40	5.6	34.2	20 32 24.6	2 35.0	
9	23 July '64	19 08 06.6	59.9N	149.2W	55	5.4	35.6	19 15 01.0	2 27.2	

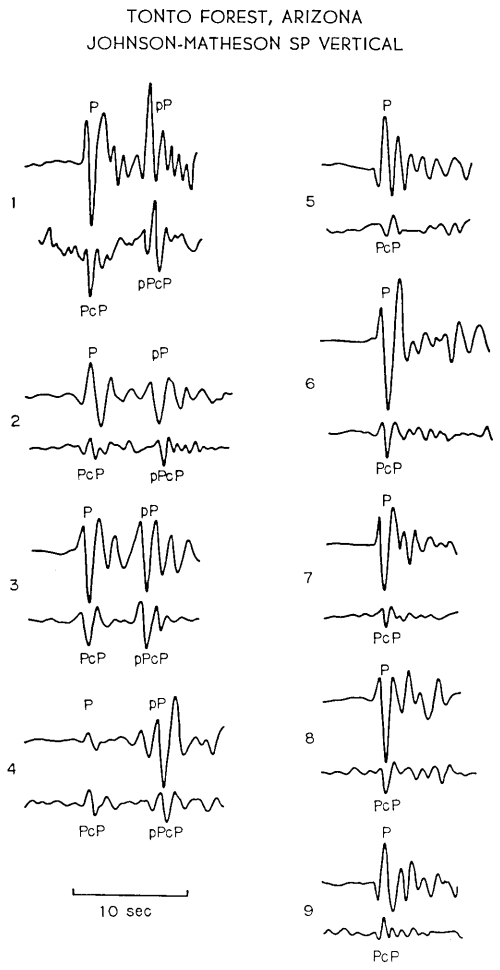

Fig. 1. Vertical component of *P*, *PcP*, *pP*, and *pPcP* phases reproduced from TFSO seismograms. Numbers are referred to those in Table 1.

Method of Analysis

The method is essentially the same as that discussed in the previous paper [*Kanamori*, 1967*a*]. The frequency spectrum of *P* phase at the station is

$$P(f)=kS(f)T(f)I(f)\exp(-2\pi if\tau)\exp\left[-\pi f\int_{\sigma_P}\frac{ds}{Q_\alpha V_P}\right] \qquad (1)$$

where $S(f)$, $T(f)$, and $I(f)$ are the source spectrum, crustal transfer function and instrument response respectively. k is the amplitude diminution factor. $\exp(-2\pi i f\tau)$ represents the propagation delay, where τ is the travel time. $\exp\left[-\pi f\int_{c_P}\frac{ds}{Q_\alpha V_P}\right]$ represents the effect of absorption by the medium, where Q_α and V_P are the specific quality factor and velocity for P waves as a function of depth. The integration is performed along the P phase path C_P. Similarly, the spectrum of PcP phase is,

$$PcP(f)=k'S(f)T'(f)I(f)\exp(-2\pi i f\tau')\exp\left[-\pi f\int_{c_{PcP}}\frac{ds}{Q_\alpha V_P}\right] \quad (2)$$

where k', $T'(f)$ and τ' are the corresponding quantities for the PcP phase. We assumed that the relative spectrum at the source is isotropic, and that the reflection at the core boundary does not affect the spectral structure. Since the angles of incidence at the base of the crust of P and PcP phases are about 37° and 11.7° at $\Delta=35°$ respectively, the crustal effects which are represented by $T(f)$ and $T'(f)$ are significantly different. Following *Haskell* [1962] we calculate the crustal transfer functions for two crustal models given in Tables 2 and 3.

Table 2. Crustal model used for the calculation of the transfer correction. Standard continental crust

	Thickness	P wave velocity	S wave velocity	Density
1st layer	11.0 km	6.10 km/sec	3.50 km/sec	2.70 g/cm³
2nd layer	9.0	6.40	3.68	2.90
3rd layer	18.0	6.70	3.94	2.90
Half space	∞	8.15	4.75	3.30

Table 3. Crustal model used for the calculation of the transfer correction. Standard continental crust with sediment

	Thickness	P wave velocity	S wave velocity	Density
1st layer	2.0 km	3.00 km/sec	1.66 km/sec	2.35 g/cm³
2nd layer	9.0	6.10	3.50	2.70
3rd layer	9.0	6.40	3.68	2.90
4th layer	18.0	6.70	3.94	2.90
Half space	∞	8.15	4.75	3.30

In order to correct for the crustal effect the following procedure is adopted. From (1) and (2) we have

$$\frac{|P(f)/T(f)|}{|PcP(f)/T'(f)|}=\frac{k}{k'}\exp(-\pi fS), \tag{3}$$

$$S=\int_{o_P}\frac{ds}{Q_\alpha V_P}-\int_{o_{PcP}}\frac{ds}{Q_\alpha V_P}. \tag{4}$$

Here S represents the differential effect of attenuation on P and PcP phases which is to be determined. In order to estimate $|P(f)/T(f)|$, and $|PcP(f)/T'(f)|$ we first define the inverse crustal transfer responses $t^{-1}(t)$ and $t'^{-1}(t)$ by taking the inverse Fourier transform of $1/T(f)$ and $1/T'(f)$ respectively. The inverse transfer response is such that, when applied to the bottom of the cust, it gives rise to an impulsive displacement at the surface after the transmission through the crust. The

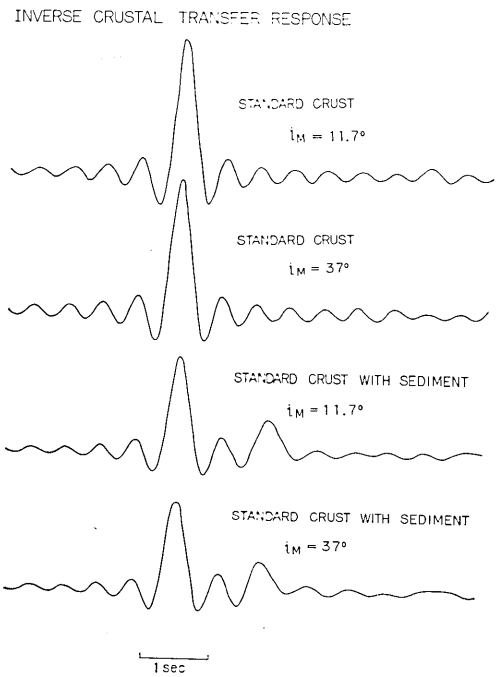

Fig. 2. Inverse crustal transfer responses with an arbitrary vertical scale for two crustal models given in Tables 2 and 3. i_M is the angle of incidence at the base of the crust. $i_M=37°$ and $i_M=11.7°$ correspond to P and PcP phases respectively. Cut-off frequency is 2 cps.

inverse transfer responses $t^{-1}(t)$ ($i_M=37°$) and $t'^{-1}(t)$ ($i_M=11.7°$) calculated for two crustal models with a high frequency cut-off at 2 cps are shown in Fig. 2. For the standard crust, no distortion of waveforms occurs, while for the standard crust with sediment the main pulse is followed by reverberations which are presumably due to the sedimentary layer. We convolve $t^{-1}(t)$ with the P phase on the seismogram to remove the crustal effect. We then Fourier analyse a portion of the convolved P phase using the time window

$$w(t)=0.54+0.46\cos\frac{\pi t}{T_m}, \qquad |t|\leqq T_m$$
$$=0, \qquad |t|>T_m$$

centered at the arrival of the main pulse. The width of the window $2T_m$ is set at 5 sec. We denote the amplitude spectrum thus calculated by $|P'(f)|$ and use it as the estimate of $|P(f)/T(f)|$. The estimate of $|PcP(f)/T'(f)|$ is similarly calculated and denoted by $|PcP'(f)|$. We now have

$$\frac{|P'(f)|}{|PcP'(f)|}=\frac{k}{k'}\exp[-\pi fS]. \tag{5}$$

The amplitude spectrum ratio $|P'(f)|/|PcP'(f)|$ is calculated for the nine pairs of P and PcP phases given in Fig. 1 and Table 1. For the four pairs of pP and $pPcP$ phases, the same procedure is used, but the crustal effect at the reflection near the source is ignored. The average of the thirteen spectral ratios will be used for the determination of S through (5).

Although all the earthquakes have about the same focal depth and distance to TFO, the amplitude diminution factor k/k' differs from one earthquake to another, because it entirely depends on the radiation pattern at the source. Hence, the absolute amplitude ratios cannot be used. In order to determine the average frequency dependence of the spectral ratios we normalize them at the frequency of 0.8 cps before taking the average. Fig. 3 is the result with the crustal effect ignored. Figs. 4 and 5 are the results when corrections are made for the standard crust (Table 2) and for the standard crust with sediment (Table 3). Although the major features are about the same, the points are better aligned on a straight line when the correction is made for the sedimentary layer. In any case, the crustal structure does not greatly affect the results. The standard deviation of the averaged ratios at specific

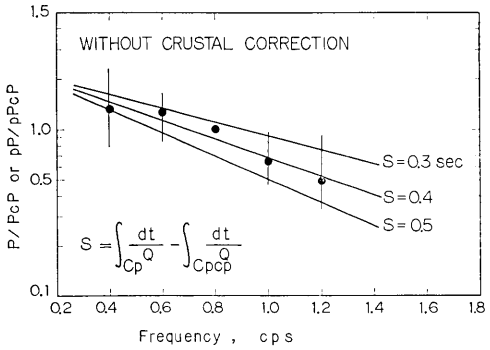

Fig. 3. Normalized spectral ratios *P/PcP* and *pP/pPcP*. The crustal effect is ignored.

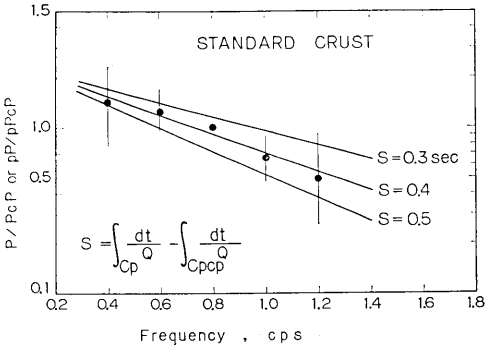

Fig. 4. Normalized spectral ratios *P/PcP* and *pP/pPcP*. The crustal effect is corrected for the standard crust given in Table 2.

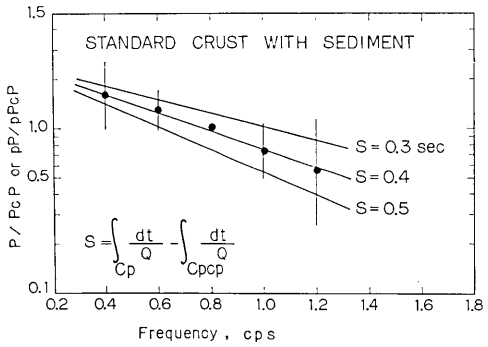

Fig. 5. Normalized spectral ratios *P/PcP* and *pP/pPcP*. The crustal effect is corrected for the standard crust with sediment given in Table 3.

frequencies is shown by the vertical lines in the figures. Slopes corresponding to several values of S are shown for the sake of comparison with the observed slope. Although the standard deviations are fairly large, the slope corresponding to $S=0.4$ sec fits the data reasonably well.

Interpretation

The value of S thus determined can be interpreted in terms of the difference of Q in the upper and the lower mantle. We define the average Q over the paths of P and PcP phases by

$$Q_P(\Delta)=\tau\Big/\int_{c_P}\frac{ds}{Q_\alpha V_P}\,,$$
$$Q_{PcP}(\Delta)=\tau'\Big/\int_{c_{PcP}}\frac{ds}{Q_\alpha V_P}\,. \qquad (6)$$

Similarly, we let $\bar{Q}_\alpha$, $\bar{Q}'_\alpha$ and $\bar{Q}''_\alpha$ be the average Q along the vertical path for the whole mantle, for the upper mantle above the deepest point of the P phase, B, and for the lower mantle below B respectively (see Fig. 6). The depth of B is about 870 km when $\Delta=35°$. We may write

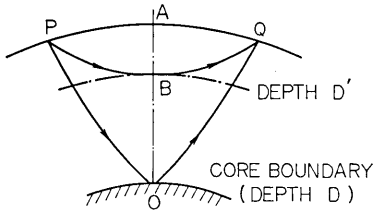

Fig. 6. Schematic illustration of ray paths of P and PcP phases.

$$\bar{Q}'_\alpha=(1+\varepsilon_1)Q_P(\Delta),$$
$$\bar{Q}_\alpha=(1+\varepsilon_2)Q_{PcP}(\Delta) \qquad (7)$$

where ε_1 and ε_2 are small quantities which represent the effect of the curvature of the ray path. For uniform Q distributions ε_1 and ε_2 are zero. Since the curvature of the ray path of the PcP phase is small at $\Delta=35°$, ε_2 is extremely small for any reasonable Q distribution. ε_1 depends only on the shape of the Q distribution within the upper mantle. Its dependence on the Q distribution is not very large. For example, ε_1 is about -0.23 for a group of Q models characterized by the MM8 model given by *Anderson et al.* [1965]. Hence, we will consider two cases; (1) $\varepsilon_1=\varepsilon_2=0$ (uniform Q for the upper mantle), and (2) $\varepsilon_1=-0.23$, $\varepsilon_2=0$ (MM8 for the upper mantle). In view of other evidence from surface wave studies [*Anderson et al.*, 1965], a preference should be given to the latter where only a general pattern of the Q distribution within the upper mantle is assumed. The former in which the Q distribution is assumed to be uniform within the upper mantle will be considered only for the purpose of comparison.

From (4), (6) and (7) we have

$$\bar{Q}'_\alpha=(1+\varepsilon_1)\tau\bar{Q}_\alpha/[\bar{Q}_\alpha S+(1+\varepsilon_2)\tau']\,. \qquad (8)$$

For $\Delta=35°$, $\tau=416$ sec and $\tau'=568$ sec. The relation between $\bar{Q}_\alpha$ and $\bar{Q}'_\alpha$ calculated from (8) for $S=0.4$ sec is given by solid curves in Fig. 7.

From the definition of $\bar{Q}_\alpha$, $\bar{Q}'_\alpha$ and $\bar{Q}''_\alpha$ the relation

$$\frac{\bar{Q}_\alpha}{\bar{Q}'_\alpha}=T_{AO}\frac{\bar{Q}''_\alpha}{\bar{Q}'_\alpha}\Big/\left[T_{BO}+T_{AB}\left(\frac{\bar{Q}''_\alpha}{\bar{Q}'_\alpha}\right)\right] \qquad (9)$$

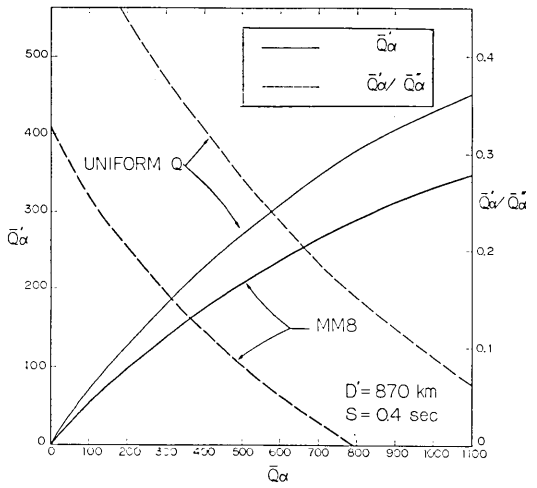

Fig. 7. Relations between $\overline{Q}_\alpha$ and $\overline{Q}'_\alpha$ (solid curves and left ordinate) and between $\overline{Q}_\alpha$ and $\overline{Q}'_\alpha/\overline{Q}''_\alpha$ (dotted curves and right ordinate) for $S=0.4$ sec. Curves designated by MM8 are the solutions when the MM8 Q distribution is assumed for the upper mantle. Curves designated by UNIFORM Q are those when Q is constant with depth in the upper mantle.

holds, where T_{AO}, T_{AB}, and T_{BO} are travel times of P waves from A to O, A to B, and B to O in Fig. 6 respectively. The relation (9) is plotted in Fig. 8 for various depths of B. Combining (8) and (9) we can derive a relation between $\bar{Q}_\alpha$ and $\bar{Q}'_\alpha/\bar{Q}''_\alpha$ which is plotted by dotted curves in Fig. 7. If the MM8 type Q distribution is preferred for the upper

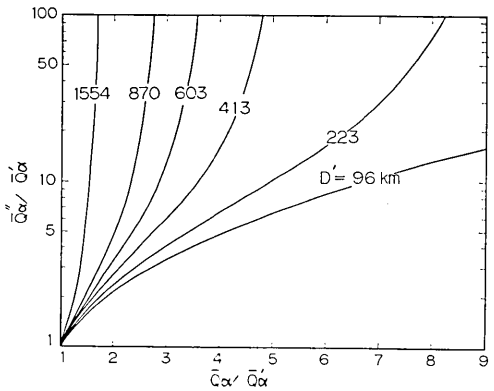

Fig. 8. Relation between $\overline{Q}''_\alpha/\overline{Q}'_\alpha$ and $\overline{Q}_\alpha/\overline{Q}'_\alpha$ for various D'. D' is the depth of the boundary of the upper and lower mantle.

limit of $\bar{Q}_\alpha$ is 800. That is, it is impossible to explain the spectral difference between P and PcP phases even with a non-attenuating lower mantle (i.e. $\bar{Q}''_\alpha = \infty$) unless $\bar{Q}_\alpha$ is smaller than 800. $\bar{Q}'_\alpha/\bar{Q}''_\alpha$ increases with decreasing $\bar{Q}_\alpha$, but it cannot be larger than 0.3. Thus the conclusions,

$$\bar{Q}_\alpha \leqq 800\,, \qquad \bar{Q}'_\alpha/\bar{Q}''_\alpha \leqq 0.3$$

immediately follow.

We can go a step further with one additional assumption. In the previous work by *Kanamori* [1967*b*] a relation between $\bar{Q}_\alpha$ and $\eta = \bar{Q}_\alpha/\bar{Q}_\beta$ was determined. If we use $1.8 < \eta < 2.5$ which is suggested by *Anderson et al.* [1965], we have $410 < \bar{Q}_\alpha < 630$ from Table 5 of *Kanamori* [1967*b*]. Combining this with the present result leads to

$$0.04 < \bar{Q}'_\alpha/\bar{Q}''_\alpha < 0.11\,,$$
$$180 < \bar{Q}'_\alpha < 240\,,$$
$$1600 < \bar{Q}''_\alpha < 6000\,.$$

Thus we can conclude that Q is about one order of magnitude larger in the lower mantle below 870 km than in the upper mantle. This substantiates the conclusion arrived at by *Anderson and Kovach* [1964], and *Kovach and Anderson* [1964] from long-period shear wave studies. The large $\bar{Q}''$ implies that the mantle below 870 km is almost perfectly elastic.

Although the uniform Q model for the upper mantle is probably not a good approximation, it may be worthwhile to take it for comparison. From Fig. 7, we then have a slightly larger ratio

$$0.22 < \bar{Q}'_\alpha/\bar{Q}''_\alpha < 0.32$$

corresponding to $410 < \bar{Q}_\alpha < 630$. This still favors the high Q lower mantle model.

Discussions and Conclusions

Two major assumptions are made in the present analysis. First of all we assumed that the relative spectrum at the source is the same for all directions. The wavelength concerned here is about 10 km while the dimension of the earthquake volume and the fault length is probably of the order of 1 km since the magnitude of the earthquakes used here is around 5.5. Therefore, this assumption is probably reasonable. However, since all the earthquakes used here are shallow and occurred at a continental margin where the crustal structure is laterally inhomogene-

ous, the possibility of the anisotropic source spectrum cannot be totally excluded.

Secondly we assumed that no spectral distortion other than those due to the attenuation and crustal layerings occurs during the transmission. A major possible source of the spectral distortion is the core boundary. If we have a detailed model of the core boundary, it can be taken into account in the analysis by the method described in the previous paper [*Kanamori*, 1967*a*]. However, uncertainties about the core boundary are as yet too great for detailed discussions to be meaningful. It is evident that any core boundary model which has any transitional nature whatsoever will increase the value of S and therefore shift the curves in Fig. 7 downward.

The crustal effect on the spectrum is small if the spectral analysis is made with a reasonably short time window. This justifies the analysis of the pP and $pPcP$ phases which ignores the crustal effect at the reflection near the source because of the uncertainties of the focal depth.

The result obtained here is consistent with that obtained in the previous analysis of P and PcP phases [*Kanamori*, 1967*a*]. There it was shown that the MM8′ Q distribution is one of the Q models which are compatible with the observed spectrums of P and PcP phases. However, to begin with, the shape of the Q distribution was assumed. Specifying the shape of the distribution is almost equivalent to assigning the value of $\bar{Q}'/\bar{Q}''$. The MM8′ Q distribution gives $\bar{Q}'/\bar{Q}''=0.09$. Thus the previous result can be compared with the particular solution of the present result with $\bar{Q}'/\bar{Q}''=0.09$. From the dotted curve in Fig. 7, we immediately have $\bar{Q}_\alpha=470$ which is in good agreement with $\bar{Q}_\alpha=435\pm120$ obtained in the previous study from an independent set of data.

The maximum value of 800, and the probable range from 410 to 630 of average Q for P waves for the whole mantle at the period of 1 sec are now compared with those estimated hitherto. *Press* [1956] obtained the value of 500 for $\bar{Q}_\beta$ ($T=11$ sec) from multiple core phases, *Otsuka* [1963] estimated $\bar{Q}_\beta$ at 300 ($T=5$ sec), *Anderson and Kovach* [1964] obtained $\bar{Q}_\beta=440$ and 510 ($T=25$ sec), and *Kovach and Anderson* [1964] found that an average Q_β of 600 for the mantle is compatible with the multiple ScS and $sScS$ data over the period range of 14 to 70 sec. *Teng* [1966] used spectrums of long-period P waves in order to estimate Q_α within the mantle. From the comparison of P and pP phases he estimated the average Q for the mantle between the earth's surface and a depth of 430 km as 60～190. He also suggested a Q_α model which has

low-Q regions in the upper mantle and near the core boundary.

The present result is in general agreement with these estimates. However, in view of the fairly abundant high frequency components contained in teleseismic signals, the present estimate of the lower limit of Q for the upper mantle ($\bar{Q}'_\alpha = 180$) seems a little too small for a representative value of the upper mantle Q. It should be noted that the present result may reflect the regional difference of Q distribution as recently suggested by *Utsu* [1966]. Utsu suggested that the abnormal distribution of seismic intensities observed in Japan may be explained in terms of regional differences in seismic wave absorption. He pointed out that a tenfold regional variation of Q in the upper mantle is possible. *Asada and Takano* [1963] also suggested regional differences of Q. Since low Q layers contribute more to the average value of Q than high Q layers, even a thin low Q layer in the mantle can appreciably reduce the average Q. Because all the earthquakes used here are from the same locality and recorded at the same station, an existence of a local low Q zone may have systematically lowered the observed Q. Dr. Don Anderson [personal communication] informed me that the mantle under TFO which is in the basin and range province is found to be more attenuating than other areas in the United States. In the basin and range province there exists evidence of low P_n velocity and high heat flow, and this is suggestive of higher mantle temperatures [*Birch*, 1966], which in turn suggests higher attenuation. It would be interesting if the regionality of Q distribution could be revealed in relation to various tectonic activities. A slightly larger value of Q for the upper mantle may be appropriate for "normal" areas.

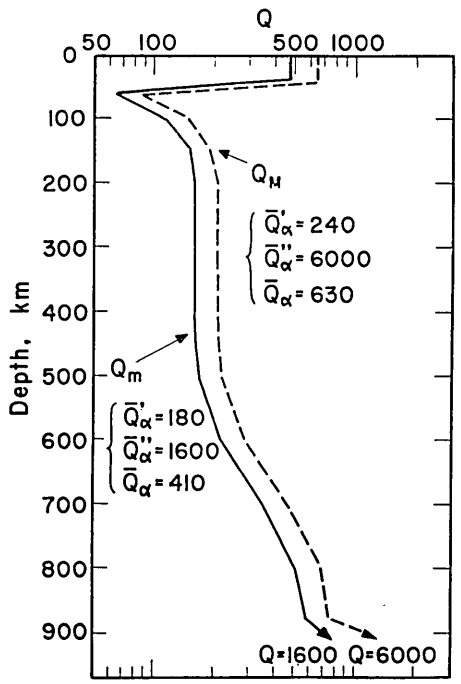

Fig.9. Minimum and maximum Q distributions Q_m and Q_M for the calculation of T/Q of *Carpenter and Flinn* [1965]. The averages of Q_m model are 180, 1600, and 410 for the upper, the lower and the whole mantle respectively. Corresponding averages for the Q_M model are 240, 6000, and 630.

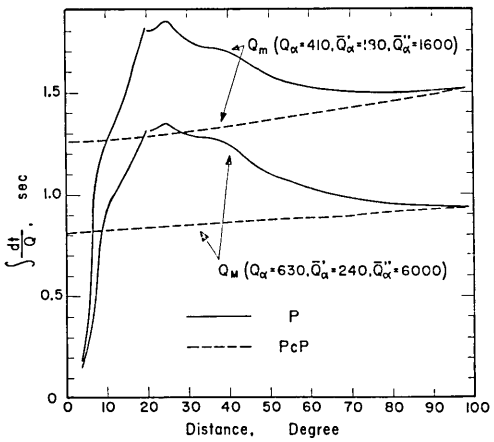

Fig. 10. The ratio of travel time to the path-average of Q, T/Q, calculated for the two Q models given in Fig. 9. Solid and dotted lines are for P and PcP phases respectively.

Carpenter and Flinn [1965] suggested that, for short-period P waves, the ratio of travel time to the path-average of Q is almost constant, about 1 sec at teleseismic distances. For comparison, we calculated the ratio for two Q models Q_m and Q_M (Fig. 9) which represent respectively the minimum and maximum Q distributions suggested here. The distribution in the upper mantle is similar to that of the MM8 model but is considerably smoothed. The lower mantle Q is assumed to be constant at 1600 and 6000 for the Q_m and Q_M models respectively. The ratios thus calculated are almost constant at $\Delta > 60°$ and are 1.5 and 1 sec for the Q_m and Q_M models respectively (Fig. 10). This is consistent with the result by Carpenter and Flinn, and a slight allowance for the relatively attenuating mantle under TFO would make the agreement even better.

The most severe limitation of the present method is the difficulty of removing the disturbing signals superposed upon P and PcP phases. This difficulty may be overcome by using as much data as possible at various stations. Records from stations having different epicenter distances will provide valuable information on the distribution of Q with depth, since P rays arriving at stations of different distances have different depths of penetration.

Acknowledgements

I am grateful to Dr. Don Anderson who read the manuscript and made valuable suggestions. Dr. T. L. Teng kindly brought to my attention a part of his thesis work in advance of publication. Comments given by Drs. M. Otsuka and R. Kovach are gratefully appreciated. Assistance by Miss T. Hirasawa in the preparation of the manuscript is also acknowledged.

References

ANDERSON, D. L., A. BEN-MENAHEM and C. B. ARCHAMBEAU, "Attenuation of seismic energy in the upper mantle", *J. Geophys. Res.*, **70**, 1441-1448, 1965.

ANDERSON, D. L. and R. L. KOVACH, "Attenuation in the mantle and rigidity of the core from multiply reflected core phases, *Proc. Natl. Acad. Sci. U. S.*, **51**, 168-172, 1964.

ASADA, T. and K. TAKANO, "Attenuation of short period *P* waves in the mantle", *J. Phys. Earth*, **11**, 25-34, 1963.

BIRCH, F., "Earth heat flow measurements in the last decade", in *Advances in Earth Science*, edited by P. M. Hurley, pp. 403-430, MIT Press, Cambridge, 1966.

CARPENTER, E. W. and E. A. FLINN, "Attenuation of teleseismic body waves", *Nature*, **207**, 745-746, 1965.

HASKELL, N. A., "Crustal reflection of plane *P* and *SV* waves", *J. Geophys. Res.*, **67**, 4751-4767, 1962.

KANAMORI, H., "Spectrum of *P* and *PcP* in relation to the mantle-core boundary and attenuation in the mantle", *J. Geophys. Res.*, **72**, 559-571, 1967a.

KANAMORI, H., "Spectrum of short-period core phases in relation to the attenuation in the mantle", *J. Geophys. Res.*, **72**, 2181-2186, 1967b.

KOVACH, R. L. and D. L. ANDERSON, "Attenuation of shear waves in the upper and lower mantle", *Bull. Seismol. Soc. Am.*, **54**, 1855-1864, 1964.

OTSUKA, M., "Some considerations on the wave forms of *ScS* phases", *Special Contributions of the Geophysical Institute, Kyoto University*, No. 2, 415-425, 1963.

PRESS, F., "Rigidity of the earth's core", *Science*, **124**, 1204, 1956.

TENG, T. L., "Body-wave and earthquake source studies", chapter 7, Attenuation of body waves and the *Q* structure of the mantle, Thesis, California Institute of Technology, Pasadena, 1966.

UTSU, T., Regional differences in absorption of seismic waves in the upper mantle as inferred from abnormal distributions of seismic intensities", *Journal of the Faculty of Science, Hokkaido University, Series 7*, **2**, 359-374, 1966.

---

16. 上部マントルおよび下部マントルにおける P 波の減衰

地震研究所　金　森　博　雄

1964年3月28日のアラスカ地震にともなう9個の余震の P, PcP, pP, $pPcP$ のスペクトル解析を行なつて，周期1秒程度の P 波に対する Q の上部マントルと下部マントルでの相違を推定した．地殻の層構造のスペクトルにおよぼす影響はハスケルの方法によつてのぞいた．P と PcP，および pP と $pPcP$ の相対スペクトル比からマントル全体での P 波に対する Q の平均，$\overline{Q}_\alpha$，の最大値は800と推定される．870 km より浅い部分のマントルについての Q の平均，$\overline{Q}'_\alpha$，と870 km より深い部分のマントルについての Q の平均，$\overline{Q}''_\alpha$，の比，$\overline{Q}'_\alpha/\overline{Q}''_\alpha$，はたかだか0.3である．今までに推定されている $\overline{Q}_\alpha$ と $\overline{Q}_\alpha/\overline{Q}_\beta$ ($\overline{Q}_\beta$ はマントル全体についての S 波の Q の平均) の関係および，表面波の減衰から推定される値 $1.8<\overline{Q}_\alpha/\overline{Q}_\beta<2.5$ を用いると，$\overline{Q}_\alpha$, $\overline{Q}'_\alpha$, $\overline{Q}''_\alpha$，および，$\overline{Q}'_\alpha/\overline{Q}''_\alpha$ の範囲はそれぞれ，$410<\overline{Q}_\alpha<630$，$180<\overline{Q}'_\alpha<240$，$1600<\overline{Q}''_\alpha<6000$，および，$0.04<\overline{Q}'_\alpha/\overline{Q}''_\alpha<0.12$ と推定される．